Electronic Supplementary Material (ESI) for RSC Advances.
This journal is © The Royal Society of Chemistry 2016

Supporting Information

Toward Rational Design of Palladium Nanoparticles with Plasmonically Enhanced Catalytic Performance

Anna Klinkova,[*,†] Aftab Ahmed,[§] Rachelle M. Choueiri,[†] Jeffrey R. Guest,[§] Eugenia Kumacheva[*,†]

[†] Department of Chemistry, University of Toronto, Toronto, Ontario M5S 3H6, Canada

[§] Center for Nanoscale Materials, Argonne National Laboratory, Argonne, Illinois 60439, United States

Contents

Synthesis of nanocubes

Palladium nanocubes (NCs) were synthesized using a modified procedure, which was originally reported elsewhere[1] (the method described below yields 500 times more NCs compared to the original reported protocol). Briefly, 115 mg of $PdCl_2$ was mixed with 6.5 mL of 0.2 M HCl and stirred for 3 h to obtain a clear orange solution of H_2PdCl_4, followed by dilution of this solution to 32.5 mL with deionized water to make 20 mM H_2PdCl_4 solution. Next, to prepare Pd seeds, 91.2 mg of cetyltrimethylammonium bromide (CTAB) was dissolved in 20 mL of deionized water in a 25 mL glass vial equipped with a stirring bar. The solution was heated to 95 °C under stirring, followed by the addition of 0.5 mL of 20 mM H_2PdCl_4 solution. After 5 min of stirring, 40 µL of 0.4 M ascorbic acid solution was quickly added. The reaction mixture was stirred for 10 min at 95 °C, then cooled down to 30 °C and allowed to age for 1 h. Meanwhile, the growth solution containing 90 g of CTAB in 900 mL of deionized water and 32 mL of 20 mM H_2PdCl_4 was prepared and stored in a water bath at 45 °C. Next, 20 mL of aged Pd seeds was added to the growth solution under vigorous stirring, followed by the addition of 25 mL of 0.4 M ascorbic acid. The resulting mixture was left undisturbed for 12 h at 45 °C. After 12 h, the resulting Pd NCs settled on the bottom of the flask. After decantation of the supernatant, the sediment was redispersed in deionized water, the solution was centrifuged at 5000 g for 15 min at 27 °C to remove CTAB access and re-dispersed in deionized water to obtain a concentrated 2.23 nM stock solution of Pd NCs.

Synthesis of nanocubes with protruded edges

Palladium nanocubes with protruded edges (PE-NCs) were synthesized by scaling up the two-step procedure reported elsewhere.[2] Briefly, 29 mg of $PdCl_2$ was mixed with 1.625 mL of 0.2 M HCl and stirred for 3 h to obtain a clear orange solution of H_2PdCl_4, followed by dilution of this solution to 8.125 mL with deionized water to make 20 mM H_2PdCl_4 solution. Next, to prepare Pd seeds, 45.6 mg of CTAB was dissolved in 10 mL deionized water. The solution was heated to 95 °C under stirring, followed by the addition of 0.25 mL of 20 mM H_2PdCl_4 solution. After 5 min of stirring, 80 µL of 0.1 M ascorbic acid solution was quickly added, the reaction mixture was stirred for 10 min at 95 °C, then cooled down to 30 °C and allowed to age for 1 h. Meanwhile the growth solution containing 22.5 g of CTAB in 225 mL of deionized water, 2.5 mL of 10 mM CuSO4 solution and 8 mL of 20 mM H_2PdCl_4 was prepared and stored in a water bath at 45 °C. Next, 5 mL of aged Pd seeds was added to the growth solution under vigorous stirring, followed by the addition of 25 mL of 0.1 M ascorbic acid. The resulting mixture was left undisturbed for 12 h at 45 °C. After 12 h, the resulting Pd NCs with protruded edges settled on the bottom of the flask. After decantation of the supernatant, the sediment was redispersed in deionized water, the solution was centrifuged at 5000 g for 15 min at 27 °C to remove CTAB access and re-dispersed in deionized water to obtain a concentrated 2.23 nM stock solution of Pd NCs.

Synthesis of Au/Pd core-shell nanocubes

Au nanocubes were synthesised using a modified seed-mediated method reported elsewhere.[3] A solution of freshly prepared, ice-cold $NaBH_4$ in deionized water (10 mM, 0.6 mL) was added under stirring to a solution prepared by mixing aqueous CTAB (0.1 M, 9.833 mL) and $HAuCl_4$ (15 mM, 0.167 mL) in a 20 mL scintillation vial. After 2 min stirring, the pale yellow mixture was left undisturbed for 2 h at room temperature. This seed solution was then diluted to 100 mL with deionized water in the Erlenmeyer flask. In another flask, a growth solution was prepared by combining aqueous solutions of CTAB (0.24 M, 4 mL) with $HAuCl_4$ (15 mM, 0.133 mL) and ascorbic acid (0.1 M, 3 mL). The resulting clear solution was subsequently diluted to 50 mL with deionized water. To this solution, 0.6 mL of the diluted seed solution was added, the resulting mixture was vigorously shaken and then left undisturbed for 12 h at room temperature. Excess CTAB from this solution was removed by using two cycles of centrifugation (15500 g, 20 min, 27 °C), removing the supernatant and redispersing the nanoparticle precipitate in 50 mL of deionized water. The resulting NP solution was subsequently mixed under vigorous stirring with 1.5 mL of 0.1 M NaBr, 16 mL of 0.1 M cetylpyridinium chloride, 50 mL of deionized water, 2.5 mL of 15 mM $HAuCl_4$, and 5 mL of 0.1 M ascorbic acid. The solution was stirred for 10 sec at room temperature, then transferred into water bath at 30 °C, and left undisturbed for 1 h. The resulting Au NCs were centrifuged once at 6000 g to remove the excess of surfactant and redisperced in the same volume of deionized water.

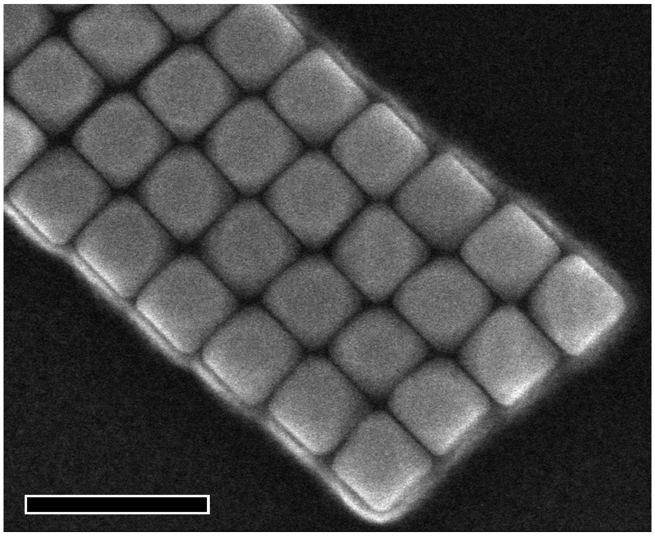

Figure S1. SEM image of Au nanocubes used as cores for CS-NCs. Scale bar is 100 nm.

To synthesize Au/Pd core-shell nanocubes, 125 mL of 0.1 M CTAB solution was mixed with 1.25 mL of 20 mM H_2PdCl_4 and 1.25 mL of 0.1 M ascorbic acid under stirring, followed by the addition of 125 mL of Au NCs. After stirring for 30 sec, the reaction mixture was transferred into water bath at 30 °C, and left undisturbed for 12 h. The resulting solution of Au/Pd core-shell NCs was then centrifuged at 4000 g for 15 min at 27 °C to remove the excess of surfactant and redispersed in deionized water to obtain a 2.23 nM stock solution of Au/Pd core-shell NCs.

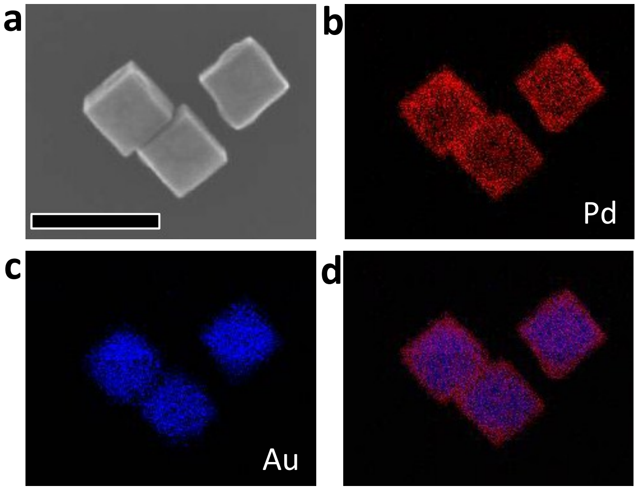

Figure S2. Characterization of the structure of CS-NCs. SEM (a,b) and corresponding EDX mapping images demonstrating a core-shell structure of Au/Pd NCs (c-e) with an elemental map of Pd (b), Au (c), and a merged elemental map (d). Scale bars are 100 nm.

Characterization of Pd and Au/Pd NPs

The NCs were characterized by scanning electron microscopy (SEM) and energy dispersive X-ray (EDX) analysis. A droplet of a dilute solution of Pd or Au/Pd NCs water was deposited onto a carbon-coated copper grid. Following solvent evaporation, the NCs were imaged using Hitachi S-5200 microscope operating at 20 kV and equipped with an EDX detector. The optical properties of the NCs were characterized by acquiring extinction spectra in a 1cm path length quartz cuvette using Cary UV-Vis-NIR spectrometer.

Determination of the concentration of NCs in solution

The concentration of the NCs in the stock solution was determined using Inductively Coupled Plasma Atomic Emission Spectroscopy (ICP-AES). 50 µL of the stock NC was mixed with 0.5 mL of aqua regia, equilibrated overnight at room temperature and subjected to a 20-fold dilution with deionized water. The concentration of Pd ions in the resulting solution was determined using ICP-AES. To convert the concentration of Pd into the concentration of NCs, we calculated the number of Pd atoms in a NC or the shell of a core-shell NC. The average dimensions of the NCs were determined by the analysing SEM images.

Catalytic experiments

The reduction of 4NP was carried out in a quartz cuvette with an optical path length of 1 cm. A small Teflon stirring bar was placed in the cuvette. A mixture of 0.2 mL of 0.5 M $NaBH_4$ solution, 0.03 mL of 10 mM 4-nitrophenol solution, and 2 mL deionized water was prepared. Then, 0.1 mL of Pd NCs, Pd PNCs or Au/Pd NCs stock solution was added to this mixture to give the concentration of 0.05 nM. The reaction was performed under stirring. The kinetics of the reaction was studied optically using Cary 5000 UV-Vis-NIR spectrometer equipped with Peltier thermostated cell holder set at 25 °C and equipped with a temperature probe accessory with a ±0.3 °C accuracy in temperature measurements; the reactions were run at least three times for each system and each condition (error bars in Figure 3 b-d correspond to standard deviation of these experiments). Continuous wave diode lasers with power of 0.7 W were utilized for photoexcitation of NCs at 450 nm (3 mm diameter, 10^4 mW/cm^2) and 532 nm (2 mm diameter, 1.5×10^4 mW/cm^2). The illumination introduced vertically from the top of the cuvette. Based on the beam diameters above, the illuminated area (and therefore illuminated volume) comprised 7% and 3% of the reaction mixture in the case of 450 nm and 532 nm laser, respectively. No change in temperature of the reaction mixture was observed during the reactions. Prior to these experiments, we verified that in the NP-free system, the concentration of 4NP remained constant for at least 2 h, both in the dark and under illumination. Warning: appropriate personal laser protection must be used.

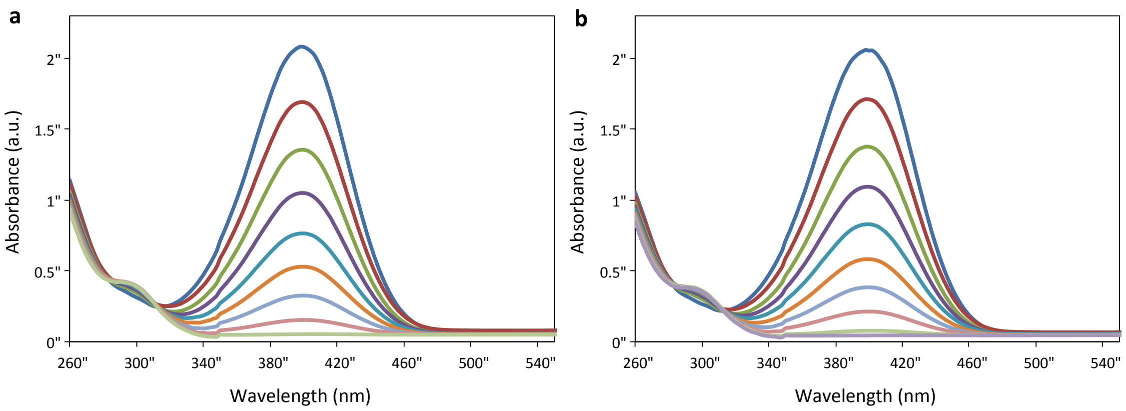

Figure S3. Evolution of the absorption spectra in the course of 4NP reduction using PE-NCs (a) and CS-NCs (b). The spectra was acquired at 1 min intervals.

Electromagnetic simulations

3D finite difference time domain simulations were carried out to investigate the optical properties of various NC geometries studied in this work. Absorption and scattering cross-sections were calculated using the formalizm of total-field-scattered-field in FDTD. Extinction cross-section is obtained from the summation of absorption and scattering cross-sections. The simulation domain was terminated with a perfectly matched layer (PML) to minimize the reflections from domain boundries. The geometries were discretized using a mesh size of 0.3 nm.

Figure S4 shows the extinction cross-section of core-shell NCs for varying core size along with that of pure Au and Pd NC. Contribution of absorption in both Au and Pd can be clearly seen for core side longer than 40 nm.

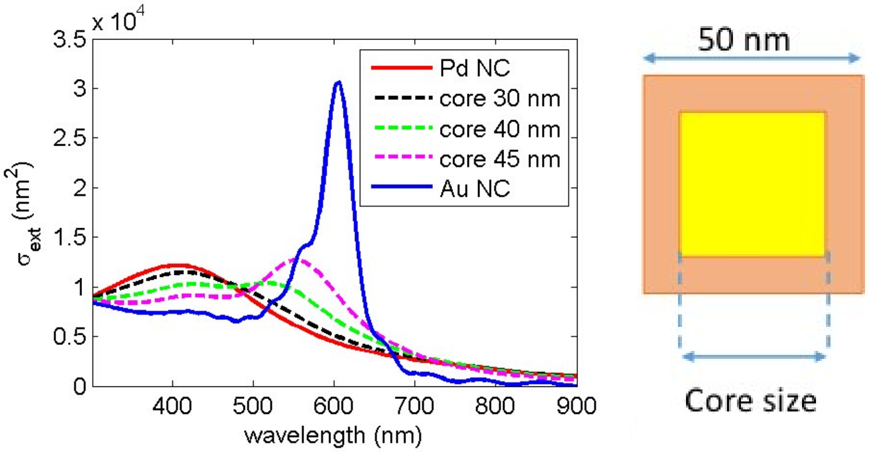

Figure S4. Evolution of extinction spectra of CS-NCs with 50 nm side length with increasing size of the core. The core and shell materials are Au and Pd respectively. Extinction spectra of pure Au and Pd NC of 50 nm side length are also plotted for comparison.

The displacement field D and electric field E are linked via polarization P as $D=\varepsilon_0 E+P$, where ε_0 is the free space permittivity. Further, $\nabla\cdot P=-\rho$, combined with charge conservation $\nabla\cdot J=-\partial\rho/\partial t$ yields the relation relating current density J and P via ($J=\partial P/\partial t$), where ρ is the charge density. These relations along with the complex permittivity of the metal ($\varepsilon=D/E$) allowed for the calculation of current density.

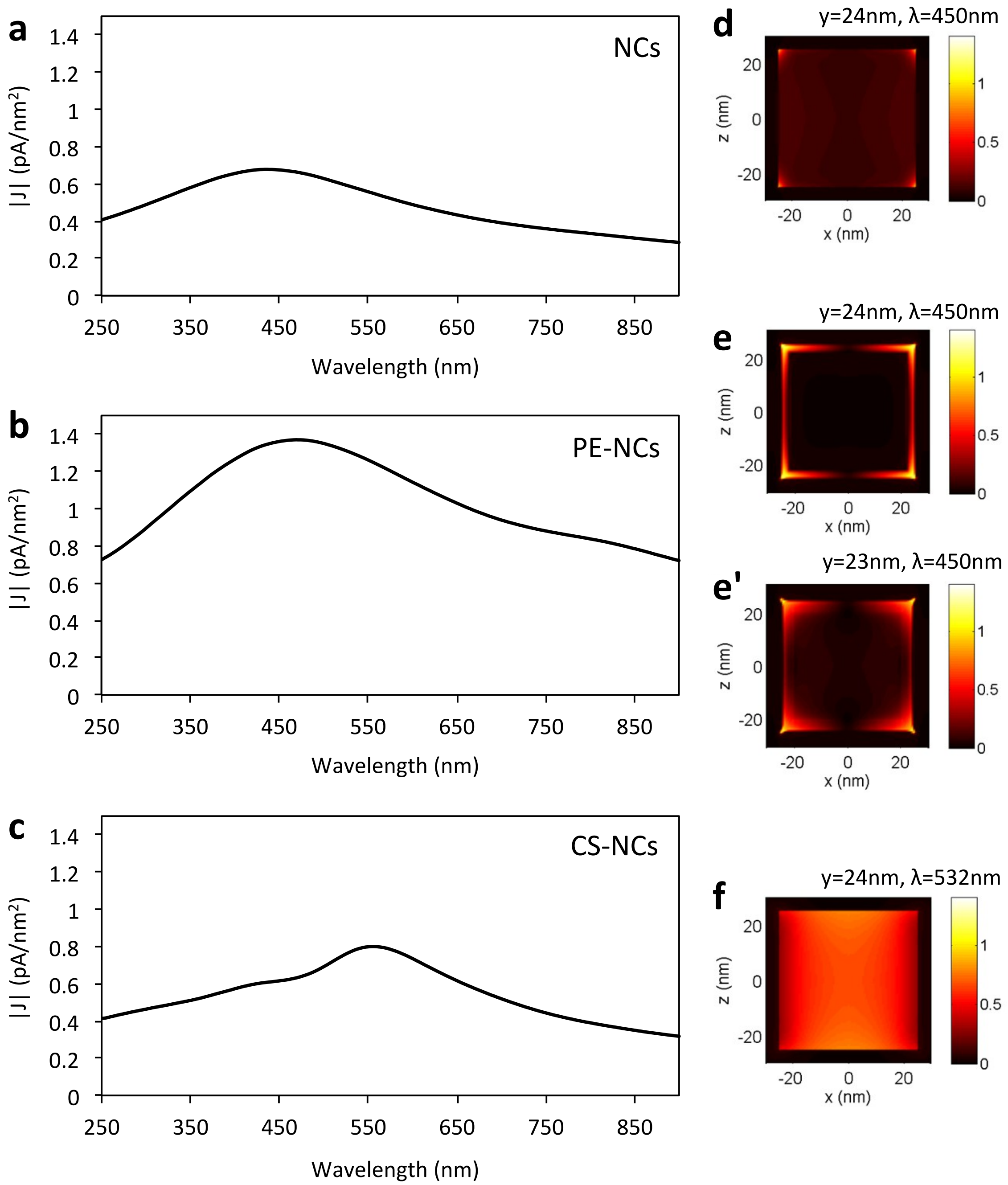

Figure S5. (a-c) Average current density profiles over the whole surface of NCs (a), PE-NCs (b), and CS-NCs (c) as a function of excitation wavelength. (d-f) Current density distribution maps for NCs (d), PE-NCs (e, e'), and CS-NCs (f) shown in xz cross section, y position of the cross section is indicated on the figure (NP center's coordinate is x,y,z=0); incident plane wave is x-polarized. Scale for J in (d-f) is logarithmic.

Consideration of photothermal heat generated by studied NPs

Under the assumption that photothermal heating is the only mechanism responsible for the increased catalytic rates, the activation energy of the reaction under plasmonic excitation should be the same as in dark. Under this assumption, the activation energy can be then used to evaluate the local photothermally induced change in temperature in the neighbourhood of the NPs. We note that in the experiments the temperature of the reaction system was maintained constant at 25.0 +/- 0.2°C, as it was thermostated. To determine activation energies of the 4NP reduction using NCs, PE-NCs, and CS-NCs, we conducted the reaction 4NP → 4AP in dark at different temperatures. The Arrhenius plots yielded the activation energies, Ea, of the reaction catalyzed by NCs, PE-NCs, and CS-NCs were 13.2, 13.2, and 12.6 kcal/mol, respectively. Based on these activation energies, the average local temperature change that would correspond to the changes in reaction rates observed could be up to 10°C (according to the Arrhenius equation, $ln\frac{k_2}{k_1}=\frac{E_a}{R}(\frac{1}{T_1}-\frac{1}{T_2})$). The highest temperature increase of 10.3°C, compared to the reaction in dark, corresponds to the 4NP → 4AP reaction performed on PE-NCs under 450 nm laser illumination (Arrhenius plot and corresponding reactions at different temperatures performed in dark are shown on Figure S6).

However, experimental and theoretical studies of plasmon mediated NP heating have demonstrated that under illumination on the order of 10^2 mW/cm^2, maximum transient temperature increases of only $\sim 10^{-2}$ K can be achieved[4,5]. Then if the rate of a thermal reaction doubles with a 10 K increase in reaction temperature, an illumination intensity of 10^6 mW/cm^2 would be necessary to produce a 2-fold increase in the reaction rate due to photothermal heating. In our experiments, illumination intensities on the order of 10^4 mW/cm^2 were used, which is still lower than would be required to explain reaction rate increase solely by plasmonic heating effect. In addition, only a fraction of the reaction volume was illuminated by the laser (3% and 7% in the case of 532 nm and 450 nm laser, respectively), thus the rate enhancement under the illumination of the whole reaction volume can be expected to be considerably higher. Therefore, while the photothermal heating mechanism should be considered in the explanation of photocatalytic reaction mechanisms on illuminated plasmonic NPs, this mechanism may not play a major role in inducing chemistry in the experiments.

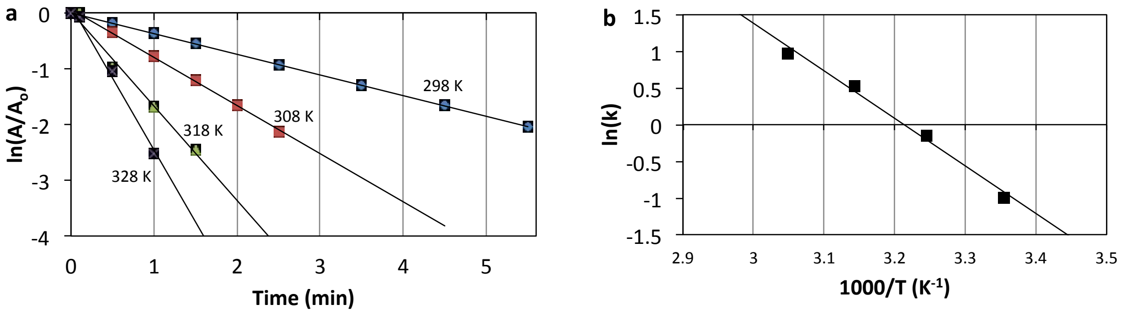

Figure S6. Determination of activation energy of 4NP → 4AP in the presence of PE-NCs. (a) Linear dependence between reaction time and the natural logarithm of absorption ratio (A is a current absorption of 4NP, and A_o is initial absorption of 4NP at the beginning of the reaction) at different reaction temperatures. (b) Arrhenius plot of the between the natural logarithm of rate constant and reaction inverse reaction temperature.

References

1. Niu, W.; Zhang, L.; Xu, G. *ACS Nano* **2010**, *4*, 1987–1996.
2. Niu, W.; Zhang, W.; Firdoz, S.; Lu, X. *Chem. Mater.* **2014**, *26*, 2180–2186.
3. Chen, H.; Sun, Z.; Ni, W.; Woo, K. C.; Lin, H.-Q.; Sun, L.; Yan, C.; Wang, J. *Small* **2009**, *5*, 2111–2119.
4. Christopher, P.; Xin, H.; Linic, S. *Nat. Chem*. **2011**, *3*, 467−472.
5. Govorov, A. O.; Richardson, H. H. *Nano Today* **2007**, *2*, 30−38.